Hindawi Publishing Corporation
Advances in Optical Technologies
Volume 2015, Article ID 581381, 5 pages
http://dx.doi.org/10.1155/2015/581381

Research Article

Robust Discrimination between Single Gold Nanoparticles and Their Dimers in Aqueous Solution for Ultrasensitive Homogeneous Bioassays

Jun Kobayashi, Yukari Takeshita, Naoto Mizuno, Keio Esashika, and Toshiharu Saiki

Graduate School of Science and Technology, Keio University, 3-14-1 Hiyoshi, Kohoku, Yokohama, Kanagawa 223-8522, Japan

Correspondence should be addressed to Toshiharu Saiki; saiki@elec.keio.ac.jp

Received 31 October 2014; Accepted 10 February 2015

Academic Editor: Saulius Juodkazis

We propose a robust method to distinguish isolated single gold nanoparticles (AuNP monomers) and their dimers under Brownian motion, a key for ultrasensitive homogeneous bioassays, including AuNP sandwich assays. To detect dimers and distinguish them from a larger number of monomers in aqueous solution, single-particle polarization microscopy was performed. For the accurate detection of individual particles, the optical anisotropy and rotational diffusion time are measured because a dimer is much more anisotropic than the nearly spherical monomer and the rotational diffusion time of a dimer is four times that of a monomer. By employing an autocorrelation analysis, we defined a measure of distinguishing that simultaneously enables high detection probability and low error probability. The detection platform offers homogeneous DNA hybridization assays and immunoassays at the subpicomolar level.

1. Introduction

Immunoassays and DNA hybridization assays are widely used in biomedical research and clinical diagnostics to detect target analytes. In these application fields, there is a considerable demand for the development of more sensitive, quantitative, rapid, and low-cost methods for target detection. To meet these requirements, gold nanoparticles (AuNPs) are attracting increasing attention as labels for probe molecules that hybridize to the target molecules [1]. This is because AuNPs are especially bright (large scattering cross section) at the plasmon resonance and chemically stable. They also provide excellent biocompatibility by employing the appropriate ligands and good tunability by varying their size and shape [2, 3].

So far, Mirkin et al. have proposed colorimetric detection methods for DNA hybridization, in which aggregation of AuNPs induced by target oligonucleotides can be monitored by a visible change in the color of the solution [4–6]. These methods take advantage of homogeneous assays in contrast to heterogeneous formats, such as southern blotting and northern blotting, which require complicated oligonucleotide immobilization and long hybridization and washing steps [7, 8]. Although the time-consuming sample handling is avoided, the detection limit in the nM range is unsatisfactory for direct detection of analytes in clinical diagnostics.

To improve the sensitivity of colorimetric detection, Huo et al. successfully combined AuNP labeling with a dynamic scattering method. Change in the average particle diameter due to the formation of nanoparticle dimers, trimers, and oligomers is sensed by quantitative correlation analysis, and the detection limit of 1 pM is demonstrated [9–11].

In this study, we propose a more robust and highly sensitive approach based on digitally counting individual AuNPs and distinguishing between isolated single AuNPs (monomers) and their dimers. We employ polarization microscopy to distinguish dimers from monomers through anisotropy measurements on individual particles [12, 13]. The difference in rotational diffusion time, which is four times larger for dimers than for monomers, is also monitored for more reliable differentiation [14, 15]. In principle, the detection limit is determined only by the uniformity of

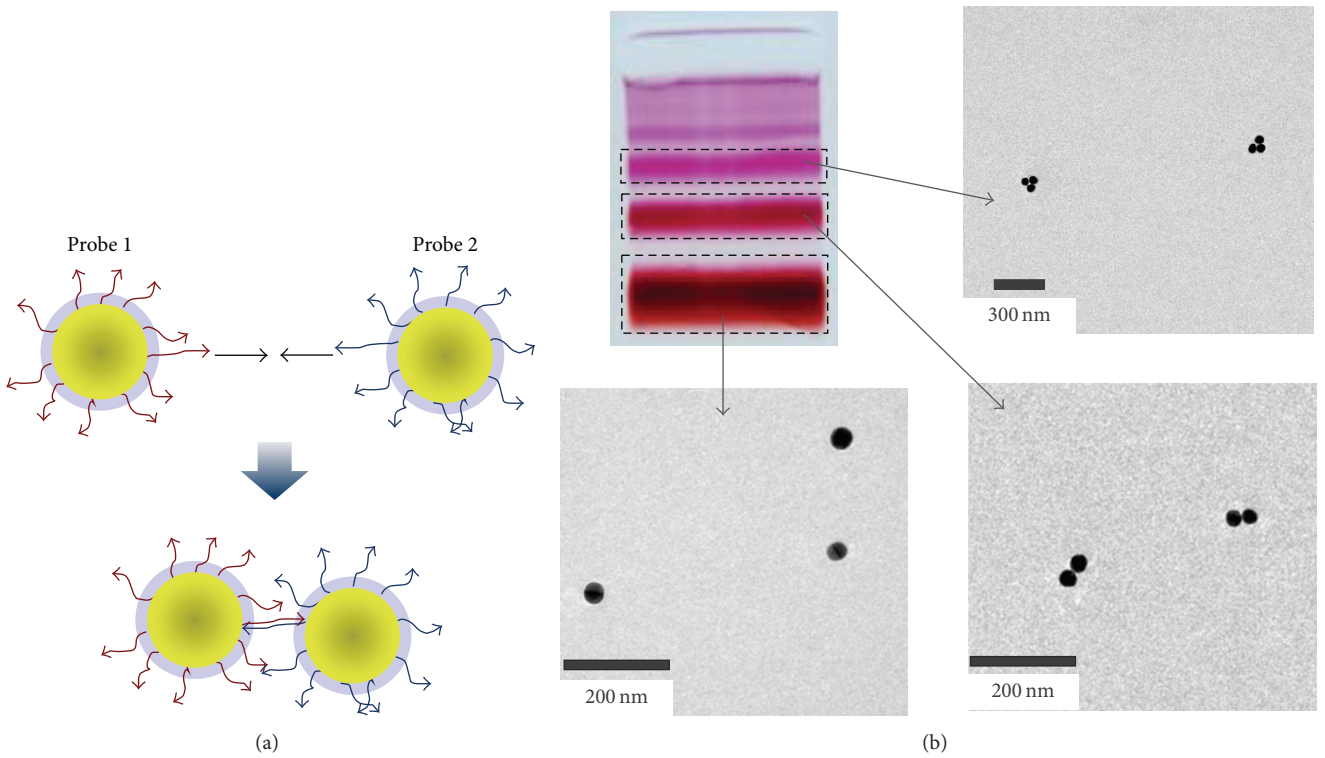

FIGURE 1: (a) Dimerization of AuNP-oligonucleotide conjugates. (b) Electrophoresis and transmission electron micrographs of monomer, dimer, and trimer particles.

the particle shape, and thus, a higher sensitivity compared to existing methods is expected.

2. Experimental

In order to assess the accuracy of AuNP differentiation, we performed polarization microscopy measurements on solutions of AuNP monomers and their dimers formed by DNA hybridization. We used a colloidal solution of AuNPs with a diameter of 40±3 nm, and the initial concentration was 170 pM (1×10^{11} particles/mL, Tanaka Kikinzoku Kogyo). The procedure for the synthesis of an AuNP dimer is as follows [16–18]. The AuNP solution was divided into two equal parts to be functionalized with two single-stranded DNA probes complementary to each other (Figure 1(a)): Probe 1: [ThiSS] 5′-AAACACTCCATCAGCGATGTAACCATG-3′ and Probe 2: [ThiSS] 5′-AAACATGGTTACATCGCT-GATGGAGTG-3′. Probe 1 and Probe 2 were added to the two AuNP solutions, respectively, at a molar ratio of 30 : 1 (DNA : AuNP). The solutions (hereinafter probe1 and probe2) were mixed well and incubated at room temperature to promote DNA hybridization (dimer formation, Figure 1(a)).

Agarose gel electrophoresis and transmission electron microscope (TEM) imaging confirmed that trimers and higher oligomers were also formed in the dimer solution as shown in Figure 1(b). The number ratio of monomer, dimer, trimer, and the higher oligomers was estimated to be 70 : 23 : 6 : 1.

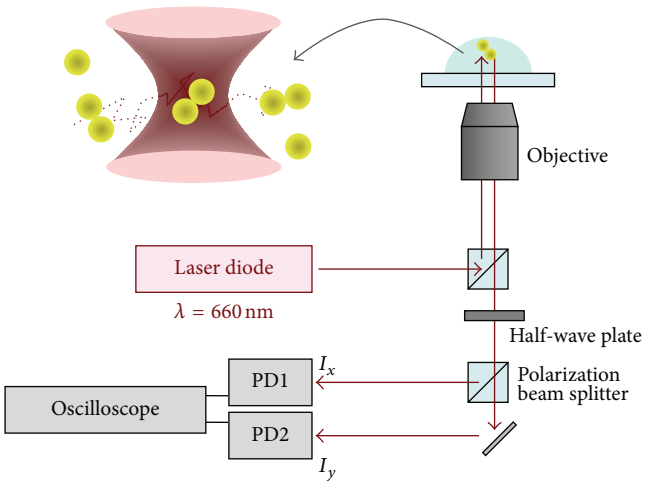

FIGURE 2: Optical measurement setup for polarization microscopy of single AuNP particles in Brownian motion in aqueous solution.

The optical measurement setup is illustrated in Figure 2. A laser diode with a wavelength of 660 nm was used as the illumination source. The laser beam (5 mW) was focused inside the AuNP solution through an objective (NA0.85, 60X) 10 μm above the glass surface. The light scattering from a single AuNP monomer or dimer moving under Brownian motion in the observation volume was collected by the same objective. A pinhole with a diameter of 100 μm was

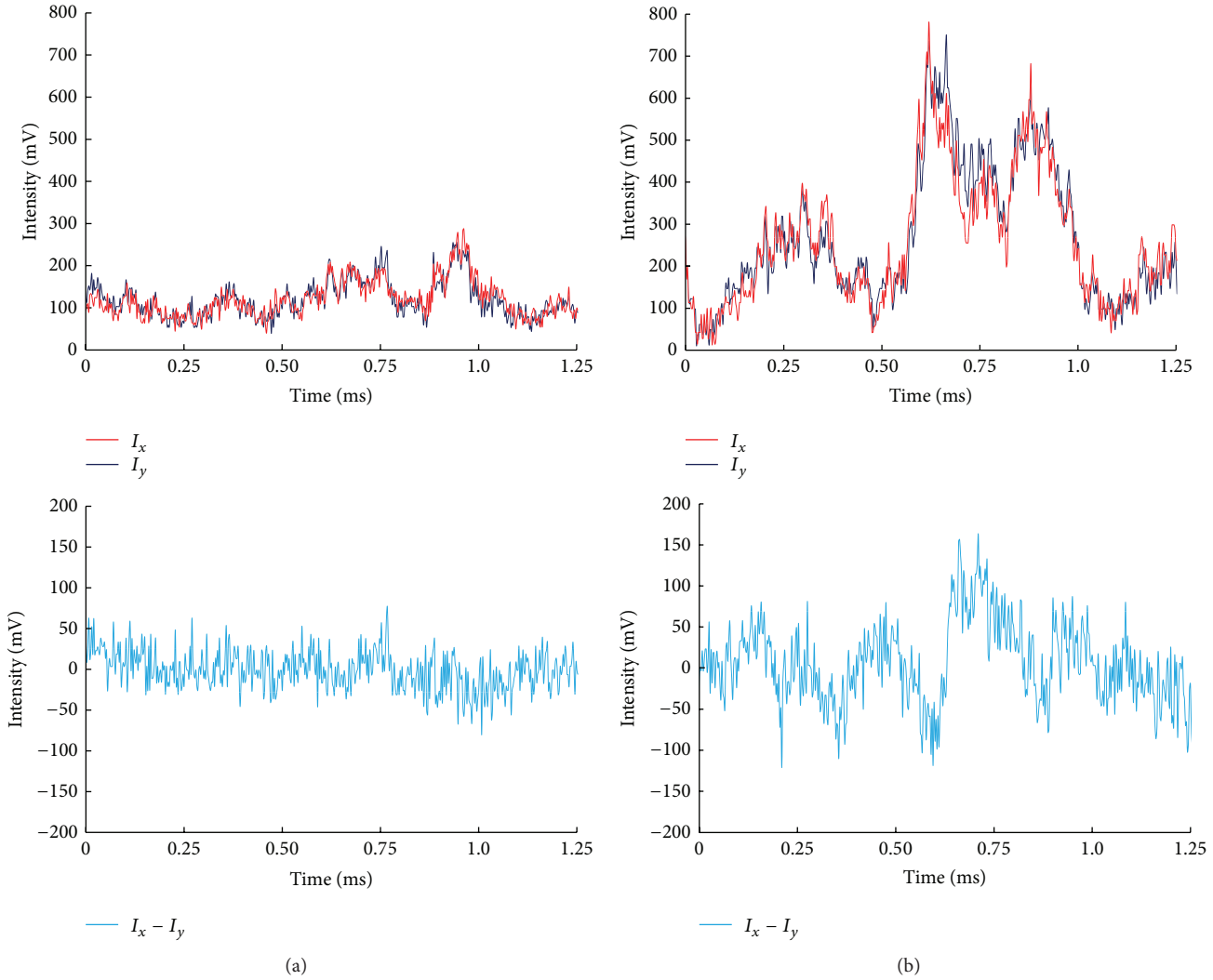

Figure 3: Representative time traces of I_x, I_y, and $I_x - I_y$ for (a) an AuNP monomer and (b) a dimer.

used to reject the out-of-focus light, thus, increasing the signal-to-noise ratio (SNR). The scattered light was split into two orthogonal x- and y-polarization components by a polarization beam splitter, and the corresponding intensities, I_x and I_y, were detected by two photodiodes and current amplifiers (10 MV/A). The difference in intensity, $I_x - I_y$, is a measure of the optical anisotropy of the AuNP monomers and dimers.

According to the calculation of plasmon coupling effect based on the quasistatic dipolar coupling approximation [19], the scattering cross section for the longitudinal plasmon mode in the dimer is expected to be approximately eight times larger than that for the monomer at the wavelength of 660 nm. Also, the polarization anisotropy defined as $(C_L - C_S)/(C_L + C_S)$, where C_L and C_S are scattering cross sections along the long and short dimer axes, is estimated to be 0.4. Here, we assumed the surface-to-surface separation of dimer to be 10 nm and employed gold dielectric function reported in [20]. Although a higher contrast in the scattering cross section between monomers and dimers and larger polarization anisotropy can be obtained at the wavelength of green light, we chose a laser diode at 660 nm due to its low cost and ready availability, which makes our approach very attractive for practical applications.

3. Results and Discussion

Figures 3(a) and 3(b) are time traces of I_x, I_y, and $I_x - I_y$ for an AuNP monomer and dimer, respectively. Figure 3(a) for the monomer contains high frequency noise, and a noticeable difference signal was not observed owing to the isotropy of the spherical particle. In contrast, for the dimer in Figure 3(b), we obtained a significant difference signal, indicating a large optical anisotropy. The slow fluctuation of the difference signal reflects the rotational motion of the dimer under Brownian motion.

To obtain a quantitative measure for differentiating monomers and dimers, we performed a statistical analysis, in which for the time trace of $I_d \equiv I_x - I_y$ we calculated an autocorrelation function, $G(\tau) = \langle I_d(t) I_d(t + \tau) \rangle$. Figure 4

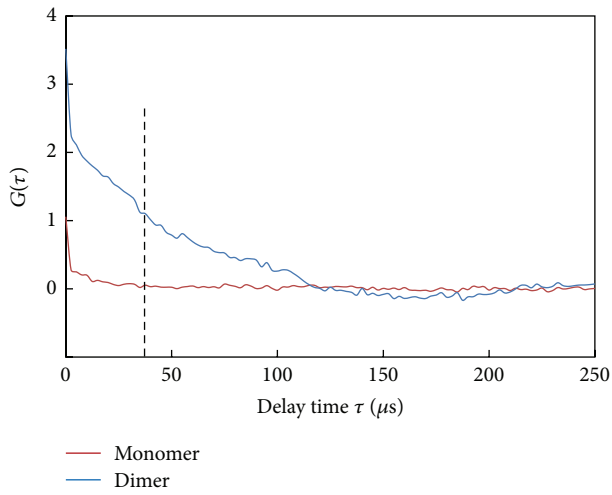

FIGURE 4: Autocorrelation curves of an AuNP monomer and a dimer calculated from the $I_x - I_y$ signals in Figure 3.

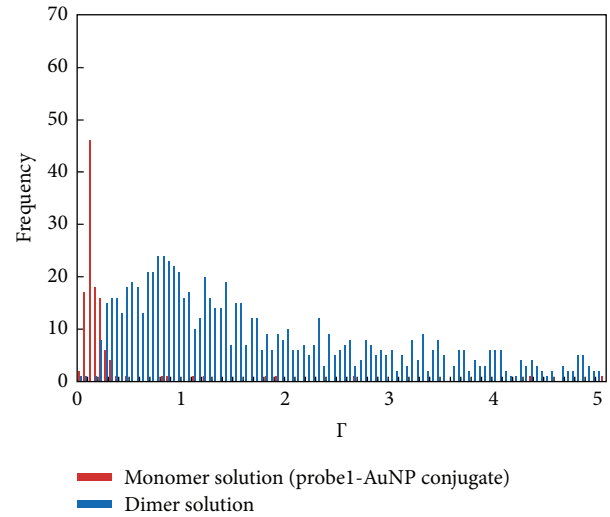

FIGURE 5: Histogram of optical anisotropy index Γ, obtained from the monomer (probe1-AuNP conjugate) and dimer solutions.

shows $G(\tau)$ curves calculated from the time traces in Figures 3(a) and 3(b). As can be seen in Figure 3, the noise frequency is higher than $1/\Delta T$, where $\Delta T = 2.5\,\mu$s is the detection time interval in the measurement (ΔT is much smaller than the rotational diffusion time). The value $G(\Delta T)$ is a good measure for differentiation, rejecting the undesired high frequency noise component, because $G(\Delta T)$ includes three important features of the dimer as compared to the monomer: (1) larger anisotropy, (2) larger scattering cross section, and (3) slower translational diffusion (longer signal duration time). To enhance the effectiveness of this measure, we also employ the decay time constant, $G(\tau)$, which reflects the difference in the rotational diffusion time between monomers and dimers. Since the diffusion time constant of the dimer is four times that of the monomer, at an appropriate time delay ΔT_{rot}, $G(\Delta T_{\text{rot}})$ will provide a more robust measure for differentiation. In this study, we adopted $\Delta T_{\text{rot}} = 40\,\mu$s to avoid the artifact of the oscillation of $G(\tau)$ due to the limited measurement time.

Figure 5 shows a histogram of $\Gamma \equiv G(40\,\mu\text{s})$ for 1,000 particles obtained from a measurement of an AuNP dimer solution in 3 min. In the same measurement time, 120 particles were detected in a monomer solution conjugated with probe1 and the distribution of Γ is also shown in Figure 5. For smaller Γ, the distributions come from both a monomer passing through the center of the observation volume which may have a larger Γ and a dimer that just grazes the observation volume boundary. By contrast, for larger Γ, dimers are dominant. However, we still have a small number of particles with a large Γ in the monomer solution. These probably originate from unexpected AuNP dimerization due to the entanglement of DNA strands. By TEM observation, we confirmed that 1% of monomers form such entangled pairs in the monomer solution. For $\Gamma > 0.5$, the number of particles obtained from the dimer solution is 910 and that from the monomer solution is only 12, which yields a ratio of 1.3%. The ratio is much smaller than the concentration ratio of dimer in the monomer solution (1%) to dimer, trimer, and higher oligomers in the dimer solution (23% + 6% + 1% = 30%). This means particles with $\Gamma > 0.5$ are identified as dimers and higher oligomers with sufficient accuracy; we can distinguish hybridized dimers (oligomers) from monomers with extremely low error probability.

Finally, we discuss the sensitivity of the proposed method under the assumption that the probe1-AuNP conjugate is the probe solution and probe2-AuNP is the target solution. By using a dissociation constant, K, for the hybridization of probe1 and probe2, we can estimate the dimer concentration $[P - T]$ to be $[T][P]/([P] + K)$, where $[P]$ and $[T]$ are the concentrations of the probe and target solutions, respectively. Here, we assume $[P - T] \ll [P]$. The probe solution contains unexpectedly large nonspherical monomers or dimers due to DNA entanglement with a probability of β. If $[P - T] > \beta[P]$, we can confirm the existence of the target. Thus, the detection limit of the target concentration is $[T] > \beta([P]+K)$. If K is sufficiently small, a reduction in $[P]$ will improve the detection limit because our strategy relies on the digital counting method. However, a reduction in $[P]$ also leads to a longer measurement time. Decreasing β is a more realistic approach that can be attempted. The current conditions, $[P] = 100$ pM and $\beta < 0.01$, will yield $[T] < 1$ pM.

4. Conclusion

By employing single-particle polarization microscopy under Brownian motion in water, sensitive and robust differentiation of isolated single gold nanoparticles (monomer) and dimers was demonstrated. We measured the optical anisotropy and the rotational diffusion time of individual particles using autocorrelation analysis. A robust measure for differentiation was defined, involving data on both optical anisotropy and rotational diffusion time. We were able to place a threshold on this measure, simultaneously achieving

sufficient detection probability and extremely low error probability.

Conflict of Interests

The authors declare that there is no conflict of interests regarding the publication of this paper.

Acknowledgments

The authors are grateful to Tanaka Kikinzoku Kogyo for providing high-quality gold nanoparticles for this study. This work was supported by JSPS KAKENHI Grant no. 24226006 and partially by Advanced Photon Science Alliance Project from MEXT.

References

[1] R. Wilson, "The use of gold nanoparticles in diagnostics and detection," *Chemical Society Reviews*, vol. 37, no. 9, pp. 2028–2045, 2008.

[2] K. Saha, S. S. Agasti, C. Kim, X. N. Li, and V. M. Rotello, "Gold nanoparticles in chemical and biological sensing," *Chemical Reviews*, vol. 112, no. 5, pp. 2739–2779, 2012.

[3] X. Huang, S. Neretina, and M. A. El-Sayed, "Gold nanorods: from synthesis and properties to biological and biomedical applications," *Advanced Materials*, vol. 21, no. 48, pp. 4880–4910, 2009.

[4] R. Elghanian, J. J. Storhoff, R. C. Mucic, R. L. Letsinger, and C. A. Mirkin, "Selective colorimetric detection of polynucleotides based on the distance-dependent optical properties of gold nanoparticles," *Science*, vol. 277, no. 5329, pp. 1078–1081, 1997.

[5] C. S. Thaxton, N. L. Rosi, and C. A. Mirkin, "Optically and chemically encoded nanoparticle materials for DNA and protein detection," *MRS Bulletin*, vol. 30, no. 5, pp. 376–380, 2005.

[6] N. L. Rosi and C. A. Mirkin, "Nanostructures in biodiagnostics," *Chemical Reviews*, vol. 105, no. 4, pp. 1547–1562, 2005.

[7] D. S. Seferos, D. A. Giljohann, H. D. Hill, A. E. Prigodich, and C. A. Mirkin, "Nano-flares: probes for transfection and mRNA detection in living cells," *Journal of the American Chemical Society*, vol. 129, no. 50, pp. 15477–15479, 2007.

[8] E. Varallyay, J. Burgyán, and Z. Havelda, "MicroRNA detection by northern blotting using locked nucleic acid probes," *Nature Protocols*, vol. 3, no. 2, pp. 190–196, 2008.

[9] E. Southern, "Southern blotting," *Nature Protocols*, vol. 1, no. 2, pp. 518–525, 2006.

[10] Q. Dai, X. Liu, J. Coutts, L. Austin, and Q. Huo, "A one-step highly sensitive method for DNA detection using dynamic light scattering," *Journal of the American Chemical Society*, vol. 130, no. 26, pp. 8138–8139, 2008.

[11] X. Liu, Q. Dai, L. Austin et al., "A one-step homogeneous immunoassay for cancer biomarker detection using gold nanoparticle probes coupled with dynamic light scattering," *Journal of the American Chemical Society*, vol. 130, no. 9, pp. 2780–2781, 2008.

[12] H. Jans, X. Liu, L. Austin, G. Maes, and Q. Huo, "Dynamic light scattering as a powerful tool for gold nanoparticle bioconjugation and biomolecular binding studies," *Analytical Chemistry*, vol. 81, no. 22, pp. 9425–9432, 2009.

[13] H. Y. Wang and B. M. Reinhard, "Monitoring simultaneous distance and orientation changes in discrete dimers of DNA linked gold nanoparticles," *Journal of Physical Chemistry C*, vol. 113, no. 26, pp. 11215–11222, 2009.

[14] B. Auguié, J. L. Alonso-Gómez, A. Guerrero-Martínez, and L. M. Liz-Marzán, "Fingers crossed: optical activity of a chiral dimer of plasmonic nanorods," *Journal of Physical Chemistry Letters*, vol. 2, no. 8, pp. 846–851, 2011.

[15] A. Tcherniak, S. Dominguez-Medina, W. S. Chang et al., "One-photon plasmon luminescence and its application to correlation spectroscopy as a probe for rotational and translational dynamics of gold nanorods," *The Journal of Physical Chemistry C*, vol. 115, no. 32, pp. 15938–15949, 2011.

[16] S. Pakdel and M. Miri, "Faraday rotation and circular dichroism spectra of gold and silver nanoparticle aggregates," *Physical Review B—Condensed Matter and Materials Physics*, vol. 86, no. 23, Article ID 235445, 10 pages, 2012.

[17] C. Sönnichsen, B. M. Reinhard, J. Liphardt, and A. P. Alivisatos, "A molecular ruler based on plasmon coupling of single gold and silver nanoparticles," *Nature Biotechnology*, vol. 23, no. 6, pp. 741–745, 2005.

[18] K. Suzuki, K. Hosokawa, and M. Maeda, "Controlling the number and positions of oligonucleotides on gold nanoparticle surfaces," *Journal of the American Chemical Society*, vol. 131, no. 22, pp. 7518–7519, 2009.

[19] H. Wang and B. M. Reinhard, "Monitoring simultaneous distance and orientation changes in discrete dimers of DNA linked gold nanoparticles," *Journal of Physical Chemistry C*, vol. 113, no. 26, pp. 11215–11222, 2009.

[20] P. B. Johnson and R. W. Christy, "Optical constants of the noble metals," *Physical Review B*, vol. 6, no. 12, pp. 4370–4379, 1972.